Boundary-Layer Meteorology (2019) 170:161–181
https://doi.org/10.1007/s10546-018-0384-0

RESEARCH ARTICLE

# Influence of Relative Humidity, Mixed-Layer Height, and Mesoscale Vertical-Velocity Variations on Column and Surface Aerosol Characteristics Over an Urban Region

**S. Ramachandran[1] · T. A. Rajesh[1] · Sumita Kedia[2]**

Received: 17 May 2017 / Accepted: 17 July 2018 / Published online: 28 August 2018


**Abstract**

Investigations into the influence of variations in relative humidity, mixed-layer height, and mesoscale vertical velocity on column and surface aerosol characteristics over urban regions are quite rare. Here we report on a comprehensive investigation that was conducted over Ahmedabad, an urban location in western India, during December 2006. In this campaign columnar and surface aerosol characteristics were measured and compared to relative humidity, mixed-layer height, and mesoscale vertical velocity to examine their influence on urban aerosol characteristics. The 500-nm aerosol optical depth was found to be approximately 0.8 between 24 and 26 December while on a cleaner day such as 7 and 18 December the aerosol optical depth was 0.1. Aerosol optical depths based on Moderate Resolution Imaging Spectroradiometer (MODIS) level-2 and level-3 data, and on in situ Sun photometer measurements, show good agreement. The scattering coefficient ($\beta_{\mathrm{sca}}$) and absorption coefficient ($\beta_{\mathrm{abs}}$) increased by a factor of 5–10 on 26 December compared to 7 December (a normal day). This latter date was characterized by a clear atmosphere, a lower mixed-layer height ($\approx$1650 m), positive vertical velocity and higher aerosol scale height ($>$3 km), while 26 December was marked with hazy and smoky conditions, a larger mixed-layer height ($\approx$2500 m), negative vertical velocity and smaller aerosol scale height ($\approx$1 km). These atmospheric conditions lead to lower and higher values of surface and columnar aerosol concentrations on 7 and 26 December respectively. A measure of spectral aerosol absorption, $\alpha'_{\mathrm{abs}} > 2$, indicating the dominance of carbonaceous aerosols from biomass/biofuel emissions (open biomass burning), is rather surprising as fossil-fuel emissions that produce strongly light absorbing carbonaceous particles usually dominate urban regions. The single-scattering albedo on both days is 0.56 and 0.67 respectively, while monthly mean hemispheric backscatter fraction $b$ and asymmetry parameter $g$ values are 0.16 and 0.53 respectively. Higher $b$ and lower $g$ values on 7 December, and lower $b$ and higher $g$ values on 26 December, provide the relative scale of variation in the amount of sub-micron aerosols that dominate on a normal/clear day vis-à-vis a smoky/perturbed day. Lower single-scattering albedo indicates the dominance of absorbing aerosols above Ahmedabad, and higher $b$ and lower $g$ values suggest the abundance of fine mode particles in aerosol size distribution. The in-depth results serve as representative inputs to modelling the column and surface characteristics, and the resultant radiative

✉ S. Ramachandran
ram@prl.res.in

Extended author information available on the last page of the article

forcing of urban aerosols influenced by variations in relative humidity, mixed-layer height, and mesoscale vertical velocity.

**Keywords** Aerosol · Dynamics · Boundary-layer height · Scale height · Urban

## 1 Introduction

Aerosols produce significant local, regional, and global climate impacts, while fossil-fuel (vehicular and industrial) emissions and biofuel/biomass burning emissions cause urban air pollution that is of local importance. Aerosols that are emitted locally can be transported from regions of high emission to clean remote locations. On a global scale aerosols affect the Earth's climate by absorption and scattering of solar and longwave radiation, and by serving as cloud condensation nuclei. Over urban regions both natural and anthropogenic sources contribute to aerosol concentration. The percentage contribution of natural versus anthropogenic sources depends on aerosol emissions, their lifetimes, extinction (scattering + absorption) characteristics, in addition to the long range transport. The optical urban-air-quality measures can vary due to a variety of factors that include, but are not limited to, local source strengths and aerosol types, remote source strengths and types, fetch region (regions from which the aerosols are transported), wind speed and direction, mixed-layer height, and mesoscale vertical velocity. Inherently it is difficult to delineate and quantify the contribution of each factor to aerosol characteristics obtained over an urban region that is influenced by both man-made and natural sources, while it is relatively less cumbersome over oceanic regions, for example, where the aerosol emissions are of one type (sea spray), and local source strengths are more or less uniform. The surface features (orography), meteorology (temperature, relative humidity), and atmospheric dynamics (mixed-layer height) also differ between ocean and land.

Studies on the influence of variations in relative humidity, mixed-layer height, and mesoscale vertical velocity on aerosol characteristics over urban regions are almost non existent in general, and in particular over India. Relative humidity can influence the size and chemical composition of aerosols; as relative humidity increases hygroscopic aerosols swell in size, thereby modifying the aerosol scattering, extinction and optical depth. Aerosol concentrations are modulated by the variations in the mixed-layer height. Mesoscale vertical-velocity variations usually confine or ventilate aerosols over a region leading to an increase or decrease in aerosol amounts, respectively. Thus, the above atmospheric variables have the potential to alter the amount, size, and the dominant type of aerosols (scattering/absorbing) as a function of altitude (surface and column) on diurnal and day-to-day time scales. For the first time, a comprehensive and systematic investigation of variation in the column aerosol properties (spectral aerosol optical depths) and in the surface aerosol characteristics (spectral scattering and absorption coefficients, black-carbon mass concentrations, and single-scattering albedo) due to the variations in relative humidity, mixed-layer effects, and mesoscale vertical velocity has been made over an urban region.

## 2 Site Description and Meteorology

Measurements of aerosol optical depths, scattering coefficients (total, $\beta_{\mathrm{sca}}$ and backscatter, $\beta_{\mathrm{backsca}}$) black-carbon mass concentrations and aerosol absorption coefficients ($\beta_{\mathrm{abs}}$) were

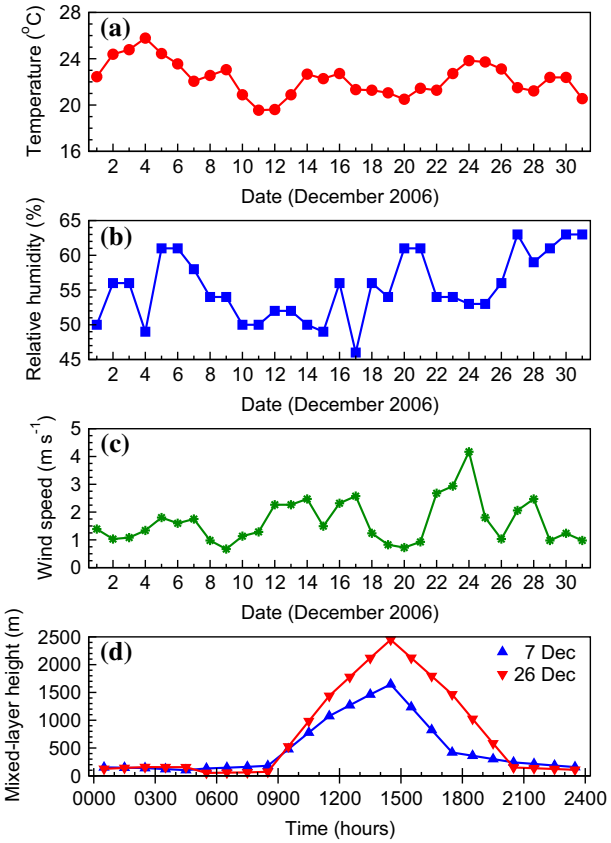


**Fig. 1** Daily mean **a** air temperature (°C), **b** relative humidity (%), and **c** surface-level wind speed (m $s^{-1}$) in December 2006 for Ahmedabad (23.03°N, 72.5°E). **d** Diurnal evolution of mixed-layer height (m) on 7 and 26 December over Ahmedabad

made during December 2006 at Ahmedabad (23.03°N, 72.5°E, 55 m above mean sea level), a densely populated, urban and industrialized city in western India. Ahmedabad has several industries and a large number of automobiles that significantly contribute to the production of aerosols including black carbon (Kedia and Ramachandran 2011). During the winter season northern and western India are frequently affected by westerly disturbances (Pasricha et al. 2003) that give rise to fog and hazy conditions, with consequent low visibility, which in turn affect the aerosol properties (Ramachandran et al. 2006). During foggy and hazy conditions, when winds are calm and vertical mixing is absent, the aerosols become trapped.

The daily mean temperatures were around 20°C in December 2006 (Fig. 1a), while the diurnal mean relative humidity and mean wind speeds were in the range of 45–65% (Fig. 1b) and 1–4 m $s^{-1}$, respectively (Fig. 1b, c). The maximum relative humidity was >85% during 24–26 December, and these days were marked with the presence of smoke, haze and dust (www.wunderground.com) in Ahmedabad. During the night (0000–0800 local time) and late evening (after 1900 local time) relative humidity was >70% during December 2006 while daytime relative humidity was in the 30–40% range.

The mixed-layer height over the continent can vary between near-zero (night) to several km (day), with the top of the layer often identified as the level of the capping temperature inversion. The mixed-layer height is low during early morning hours and gradually increases, reaching a maximum in mid-afternoon and then decreases in the evening (Stull 1988) (Fig. 1d). The mixed-layer height estimated from the Hybrid Single Particle Lagrangian Integrated Trajectory (HYSPLIT) model (Draxler and Hess 1998) using the turbulent kinetic energy profile or temperature profile can be uncertain by 250 m. The mixed-layer height calculated from the HYSPLIT model is found to exhibit diurnal and day-to-day variations over Ahmedabad (Fig. 1d). Of immediate interest, the mixed-layer is deeper on 26 December compared to 7 December (Fig. 1d) during daytime, with 7 and 26 December chosen for illustrative purposes as they show quite different mixed-layer heights (Fig. 1d), and significantly different aerosol properties that are examined further.

## 3 Measurements, Data Analysis and Approach

### 3.1 Primary Measurements

#### 3.1.1 Aerosol Optical Depths: Sun Photometer

A handheld Sun photometer was used to measure the direct solar radiation intensities at four spectral bands centered around 400, 500, 660 and 850 nm, with the bandwidth of these interference filters $\leq 10$ nm. The Sun photometer consists of an interference filter, photodiode and necessary readout electronics, with the total field of view restricted to 8°.

The governing equation for Sun photometric measurements is Beer-Lambert's law, which is expressed as

$$\tau_{\text{total}} = \frac{-1}{m}\left[\ln\left(\frac{I}{I_0}\right) - 2\ln\left(\frac{r_0}{r}\right)\right], \tag{1}$$

where $\tau_{\text{total}}$ is the total integrated columnar optical depth of the atmosphere, $I$ is the instantaneous solar radiation intensity measured by the photometer and $I_0$ is the solar radiation intensity obtained from a Langley plot extrapolated for zero airmass, $m$ is the atmospheric airmass, $r$ is the instantaneous value of the Sun–Earth distance, and $r_0$ is the Sun–Earth distance when $I_0$ values are obtained.

Sun photometric measurements were taken daily at different solar zenith angles in clear-sky conditions during December 2006, from about 0800 to 1700 local time at 15-min intervals between 1 and 31 December 2006 ($n = 20$ days). The solar radiation intensity for zero airmass ($I_0$) was obtained, using the Langley plot technique for all wavelengths, from the measurements conducted at Mount Abu (24.6°N, 72.7°E), a hill station and a relatively clean site located at a height of about 1.7 km above mean sea level (Kedia and Ramachandran 2011). These $I_0$ values were used in Beer-Lambert's law to derive the optical depths at each wavelength. The uncertainties in the optical depth measurements arise from errors in the instrument due to bias and precision, and because of ignoring the forward-scattering contribution to the measured irradiance. The aerosol optical depth ($\tau$) was obtained after subtracting the contribution from scattering due to air molecules, ozone, water vapor etc. at the respective wavelengths. All the above sources were found to cumulatively contribute an error of 3–8% to the measured aerosol optical depths in the 400–850 nm wavelength region (Kedia and Ramachandran 2011).

**Table 1** Instruments, primary atmospheric aerosol measurements made over Ahmedabad and derived parameters

| Altitude coverage | Primary measurements | Derived parameters |
|---|---|---|
| Column | *Sun photometer* | |
| | Aerosol optical depth ($\tau$) | $\tau_\lambda = \beta\lambda^{-\alpha}$, |
| | (400, 500, 660 and 850 nm) | Ångström exponent, $\alpha$, |
| | | Ångström coefficient, $\beta$ |
| Surface | *Nephelometer* | |
| | Total scattering ($\beta_{sca}$) | Ångström exponent (nephelometer), |
| | and hemispheric | $\alpha_{neph} = -\ln(\beta_{sca}(700)/\beta_{sca}(450))/\ln(700/450)$, |
| | backscattering ($\beta_{backsca}$) | Hemispheric backscatter fraction, |
| | coefficients | $b$ at 550 nm = $\beta_{backsca}/\beta_{sca}$, |
| | (450, 550 and 700 nm) | Asymmetry parameter, $g$ at 550 nm |
| Surface | *Aethalometer* | |
| | Black-carbon aerosol | Aerosol absorption coefficients, |
| | mass concentrations | $\beta_{abs} = \sigma_{abs}(\lambda)$ Black-carbon mass/C, |
| | (370, 470, 520, 590, | Aerosol absorption exponent, $\alpha'_{abs}$, |
| | 660, 880 and 970 nm) | $\beta_{abs}(\lambda) = K\ \lambda^{-\alpha'_{abs}}$, |
| | | Single-scattering albedo (*SSA*) at 550 nm, |
| | | $SSA = \beta_{sca}/(\beta_{sca} + \beta_{abs})$ |

### 3.1.2 Aerosol Scattering Coefficients: Nephelometer

An integrating nephelometer (TSI 3563, USA, Table 1) was used for measuring scattering ($\beta_{sca}$) and backscattering ($\beta_{backsca}$) aerosol coefficients at 450, 550, and 700 nm. A built-in sample heater was used during the measurements that minimized the condensation on the instrument walls caused by aerosols at high relative humidity. Aerosol scattering depends on the relative humidity since the sizes of hygroscopic aerosols increase with increase in relative humidity. The hygroscopic scaling factor expressed as the ratio of $\beta_{sca}$ at ambient relative humidity and $\beta_{sca}$ at 30% relative humidity is derived for urban aerosols. Similarly, scaling factors for $\beta_{backsca}$ have also been derived. The hygroscopic scaling factors at 450, 550, and 700 nm for urban aerosols are calculated using the log normal distribution parameters ($r_m$, mode radii and $\sigma$, width of the size distribution) given in Hess et al. (1998) from 30 to 80% relative humidity following Ramachandran et al. (2006). Hygroscopic scaling factors at 550 nm for urban aerosols are found to be 1.1 (40% relative humidity), 1.2 (50% relative humidity), 1.3 (60% relative humidity), 1.4 (70% relative humidity) and 1.7 (80% relative humidity). Hygroscopic scaling factors at 550 nm determined here are in good agreement with the mean value of $1.7 \pm 0.3$ at 80% relative humidity obtained by Charlson et al. (1984) and Hegg et al. (1996).

The nephelometer was operated at a flow rate of 20 L min$^{-1}$. The aerosol scattering coefficients were measured at a 5-min averaging time between 1 and 31 December 2006 ($n =$ 31 days), and scaled to 30% relative humidity as discussed above, using the relative humidity measured at the inlet of the nephelometer during each observation. The nephelometer was calibrated for which the instrument was adjusted to zero using a flow of particle-free air, and span calibration was performed using $CO_2$ gas. The uncertainties associated with aerosol

inlets, tubing and losses within the nephelometer were found to be insignificant for sub-micrometre particles (Clarke et al. 2002). Aerosol scattering coefficients used herein were measured over an urban area, where sub-micron particles are expected to dominate the aerosol size distribution. The nephelometer measurements have been corrected for truncation errors following Anderson and Ogren (1998) and Anderson et al. (1996); the uncertainty in $\beta_{sca}$ was estimated to be 15%.

#### 3.1.3 Black-Carbon Aerosol Mass Concentrations and Aerosol Absorption Coefficients: Aethalometer

Measurements of black-carbon aerosol mass concentrations and aerosol absorption coefficients were made at 370, 470, 520, 590, 660, 880 and 950 nm using an aethalometer (AE 31, Magee Scientific, USA, Table 1). Black-carbon mass concentrations are obtained by converting the attenuation of a beam of light transmitted through the sample collected on a filter using the calibration factors given by the manufacturer (Magee Scientific). The sources of uncertainty in black-carbon mass concentrations measured using the aethalometer arise from instrumental artifacts such as flow rate, filter spot area, and detector response. The flow rate was checked by the flow meter on a daily basis during the measurement period and the flow rate found to be quite stable. Taking into account all of these effects, the overall uncertainty in the reported black-carbon mass concentrations and absorption coefficients ($\beta_{abs}$) is estimated to be 10%.

### 3.2 Complementary Satellite Data

#### 3.2.1 Aerosol Optical Depths: MODIS Terra and Aqua

The MODerate resolution Imaging Spectroradiometer (MODIS) is a remote sensor on board two Earth Observing System (EOS) Terra and Aqua satellites. MODIS Collection 6 atmospheric daily level-2 (10 km $\times$ 10 km resolution), and level-3 ($1^\circ \times 1^\circ$ resolution) global aerosol optical depths, derived incorporating improved surface reflectance characteristics, are utilized. The error in MODIS (Terra and Aqua) derived aerosol optical depth ($\tau$) over land is $\Delta\tau = \pm 0.05 \pm 0.15\tau$ (Remer et al. 2008). The daily aerosol optical depths at 550 nm from Terra and Aqua satellites, and their mean corresponding to Ahmedabad during December 2006 are analyzed.

### 3.3 Derived Parameters

#### 3.3.1 Ångström Parameters ($\alpha$ and $\beta$)

Aerosol optical depths in the 400–850 nm wavelength range were analyzed further to determine the Ångström parameters ($\alpha$ and $\beta$) by fitting the Ångström power law (Table 1). The values of $\alpha$ and $\beta$ were estimated for an individual dataset of aerosol optical depths in the wavelength range of 400–850 nm by least-square fitting the aerosol optical depths against the respective wavelength on a log-log plot. The wavelength exponent $\alpha$ depends on the size distribution of aerosols, and $\beta$ is directly proportional to the columnar aerosol content, and is equal to the aerosol optical depth measured at 1 $\mu$m. A higher $\alpha$ value indicates the dominance of fine-mode aerosols ($\leq$1 $\mu$m in radius) in the aerosol size distribution, while a lower $\alpha$ suggests the dominance of coarse-mode aerosols ($\geq$1 $\mu$m in radius).

### 3.3.2 Ångström Exponent ($\alpha_{neph}$) of Aerosol Scattering Coefficients

The total ($\beta_{sca}$) aerosol scattering coefficients were further analyzed to determine the sizes of scattering particles (smaller or bigger) that dominate the surface-level aerosol distribution. The Ångström exponent of aerosol scattering coefficients, referred to as $\alpha_{neph}$, describes the wavelength dependence of aerosol scattering coefficients (Table 1). Smaller values of $\alpha_{neph}$ indicate the dominance of larger particles (>1 μm) in scattering, while higher $\alpha_{neph}$ arise due to the abundance of smaller particles (<1 μm) in the aerosol size distribution.

### 3.3.3 Aerosol Absorption Coefficients

The measured black-carbon mass concentrations were used to calculate the aerosol absorption coefficients ($\beta_{abs}$) following the relation given in Table 1. The wavelength dependent correction factor C (Table 1) is obtained following Bodhaine (1995). The absorption efficiency ($\sigma_{abs}$) values at 370, 470, 520, 590, 660, 880, and 950 nm are 39.5, 31.1, 28.1, 24.8, 22.2, 16.6, and 15.4 $m^2\ g^{-1}$ respectively, which were used to determine the black-carbon mass concentrations and $\beta_{abs}$ at the respective wavelengths (Ramachandran and Rajesh 2007).

### 3.3.4 Spectral Dependence of Aerosol Absorption ($\alpha'_{abs}$)

The spectral absorption of aerosols defined as $\beta_{abs}\ (\lambda) = K\ \lambda^{-\alpha'_{abs}}$ was found to follow a power law (Kirchstetter et al. 2004) (Table 1). The exponent $\alpha'_{abs}$ gives an insight into whether the absorbing aerosols are dominated by fossil-fuel or biomass/biofuel-burning emissions. Light absorption by fossil-fuel emissions was found to exhibit a relatively weak spectral dependence as compared to biomass-burning emissions (Kirchstetter et al. 2004). Values of $\alpha'_{abs}$ were determined utilizing the measured spectral $\beta_{abs}$ values (Table 1).

### 3.3.5 Single-Scattering Albedo

The single-scattering albedo (*SSA*) was determined from $\beta_{sca}$ and $\beta_{abs}$ (Table 1), with $\beta_{sca}$ at 550 nm and $\beta_{abs}$ at 555 nm (estimated by averaging the $\beta_{abs}$ measured at 520 and 590 nm) utilized to derive the SSA. The uncertainty in the SSA due to the use of aerosol scattering and absorption coefficients that are separated by 5 nm is found to be insignificant. The uncertainties in $\beta_{abs}$ and $\beta_{sca}$ contribute a maximum relative standard error of <10% in the single-scattering albedo (Ramachandran and Kedia 2011).

### 3.3.6 Hemispheric Backscatter Fraction (*b*) and Asymmetry Parameter (*g*)

The relative-humidity-corrected $\beta_{sca}$ and $\beta_{backsca}$ coefficients were used to calculate the hemispheric backscatter fraction ($b$), defined as the ratio of light scattered into the backward hemisphere ($\beta_{backsca}$) to total light scattering ($\beta_{sca}$) (Andrews et al. 2006). The angular distribution of light scattered by aerosols is represented by the asymmetry parameter ($g$) that depends on the aerosol size distribution and chemical composition. The backscatter fraction and asymmetry parameter influence the aerosol contribution to radiative forcing. In spite of its important role in radiative transfer studies, in situ measurements and estimates of the asymmetry parameter $g$ are rare, and to date there exists no direct means of measuring the aerosol asymmetry parameter $g$. Andrews et al. (2006) obtained a relation between $b$ and $g$ based on Wiscombe and Grams (1976); viz. $g = -7.143889b^3 + 7.464439b^2 - 3.96356b + 0.9893$ (Eq. 4, Andrews et al. 2006).

## 4 Results and Discussion

### 4.1 Column Aerosol Characteristics

Sun photometer, and MODIS (level-2 and level-3) aerosol optical depths track quite well with each other throughout the measurement period (Fig. 2a). Aerosol optical depths are in the 0.2–0.6 range during 1–10 December; thereafter aerosol optical depths decrease and are $\leq$0.3 up to 20 December. Then aerosol optical depth increases, and reaches a maximum value of 0.8 on 26 December, decreasing by a factor of 4 to 0.2 on 27 December (Fig. 2a). The differences in the mean low (18 December) and high (25–26 December) aerosol optical depths are larger than the uncertainties involved in estimating aerosol optical depths. Wind speed is an important factor for mixing-related changes to aerosol optical depth, in addition to long range transport (fetch and synoptic situation) and mesoscale vertical velocity (rising/sinking motion of air parcels). The mean wind speed changes from 4.2 m $s^{-1}$ on 24 December to 1 m $s^{-1}$ on 26 December (Fig. 1c), yet the aerosol optical depths are not significantly different. The ventilation coefficient, which is the product of wind speed and mixed-layer height, plays a crucial role in dispersing the pollutants and can give rise to either high or low aerosol optical depths. The ventilation coefficient can be high when wind speeds are high and/or the mixed layer is higher. In the present case, though the wind speed changes significantly the mixed layer is thicker ($\approx$2500 m) on 26 December (Fig. 1d). In addition, it should be noted that the wind speeds are near-surface, while aerosol optical depth is a columnar measure that can be influenced by other factors mentioned above. The correlation between Sun photometer and MODIS level-2 aerosol optical depths (Fig. 2b), and between Sun photometer and MODIS level-3 aerosol optical depths (Fig. 2c), is very good (the coefficient of determination ($R^2$, the square of the correlation coefficient $R$), is $\geq$0.8 in both cases). MODIS level-2 (at 10 km resolution) and MODIS level-3 (1° resolution) aerosol optical depths compare very well over Ahmedabad (Fig. 2d); however, MODIS level-3 aerosol optical depths are lower than MODIS level-2 values and in situ, ground-based Sun photometer aerosol optical depths.

The Ångström exponent ($\alpha$) (Sect. 3.3.1, Table 1) values, are in the 1.5–2 range during 1–15 December 2006, reaching their lowest value of 1.1 on 18 December. Aerosol optical depth is also the smallest on 18 December with a value of 0.1 (Table 2). When the wind speeds are low, aerosols are not properly ventilated or transported to downwind locations. Over an urban region no significant change in the local production of aerosols from anthropogenic activities, such as industrial emissions and automobile exhausts, is expected during the year. Aerosol emissions and behavior during weekday/weekend were almost the same over Ahmedabad (Bapna et al. 2013). The parameter $\beta$, which represents the columnar loading of aerosols, is about 0.1 from 1 to 10 December (Fig. 1e) and decreases thereafter with the exception of 24–26 December; $\beta$ values track well the aerosol optical depth features (Fig. 2a). The values of $\beta$ were $>$ 0.2 during 24–26 December, indicate an increase in columnar loading of aerosols (Table 2); on 26 December it is six times higher than the value obtained on 18 December (Table 2). Higher aerosol optical depths, $\alpha$ and $\beta$ obtained on 26 December indicate a significant increase in the columnar loading of both fine and coarse mode aerosols compared to 18 December.

Vertical velocity (Pa $s^{-1}$) represents the time rate of change of pressure; negative vertical velocity denotes subsidence (sinking air) motion while positive fields indicate rising (ascent) motion. Vertical velocity in the NCEP reanalysis is calculated based on the $u$ and $v$ wind components at different pressure levels using the state-of-the-art data assimilation system. The wind data ($u$ and $v$) used from the NCEP reanalysis are strongly influenced by observations,

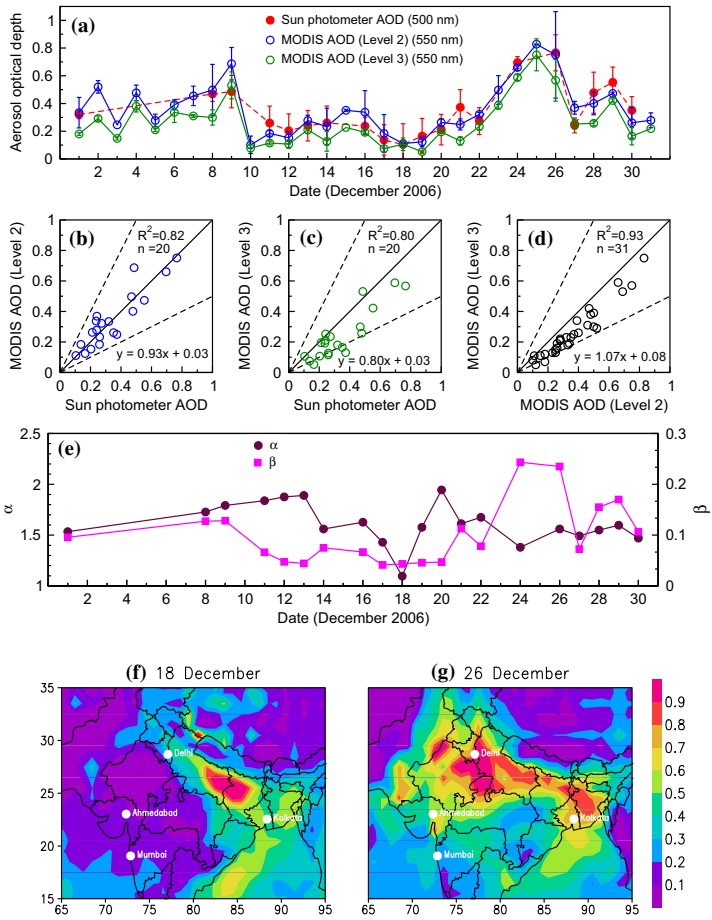


**Fig. 2** **a** Daily mean 500-nm aerosol optical depth measured in situ by the Sun photometer over Ahmedabad, 550-nm MODIS (Terra and Aqua mean) level-2 and level-3 aerosol optical depths for Ahmedabad during December 2006. Scatter plots of **b** Sun photometer aerosol optical depth (AOD) versus MODIS (Terra and Aqua mean) level-2 aerosol optical depth, **c** Sun photometer aerosol optical depth versus MODIS (Terra and Aqua mean) level-3 aerosol optical depth, and **d** MODIS (Terra and Aqua mean) level-2 aerosol optical depth versus MODIS (Terra and Aqua mean) level-3 aerosol optical depth. The coefficient of determination ($R^2$), number of data points and the regression equations are given in **b**–**d**. Solid and dotted lines correspond to 1:1 and 2:1 ratios respectively. **e** Daily mean values of Ångström parameters $\alpha$ and $\beta$ derived from spectral aerosol optical depths measured by the Sun photometer. Spatial maps of MODIS (Terra and Aqua mean) level-3 550-nm aerosol optical depths on **f** 18 December, and **g** 26 December 2006. The study location, Ahmedabad, and the cities of Delhi, Mumbai, and Kolkata are shown on the maps

and are in the most reliable class (Kalnay et al. 1996). Mesoscale vertical velocity is negative (Fig. 3a) restricting/containing aerosols over a location/region, resulting in higher aerosol amounts (24–26 December) and higher aerosol optical depths, where as positive mesoscale vertical velocity (Fig. 3a) from the surface leads to ventilation of pollutants (16–18 December), and lower aerosol optical depths. The influence of variations in the mesoscale vertical velocity on aerosol optical depths is further seen explicitly on 27 December, when the velocity becomes positive and results in lower aerosol optical depths (Fig. 3a). The regional nature of haze/smoke that led to higher aerosol optical depths over Ahmedabad is clearly visible

**Table 2** Variations in column and surface aerosol characteristics over Ahmedabad during clear, and hazy and smoky conditions

| Atmospheric conditions, values | Date(s) | Diurnal mean aerosol properties | | | | | | |
|---|---|---|---|---|---|---|---|---|
| | December 2006 | Column | | | Surface | | | |
| | | $\tau$ | $\alpha$ | $\beta$ | $\beta_{sca}$ | $\beta_{abs}$ | BC mass | *SSA* |
| Clear, low | 7, 18[a] | 0.10 | 1.43 | 0.04 | 81.5 | 64.2 | 4.3 | 0.56 |
| Hazy/smoky, high | 26 | 0.77 | 1.56 | 0.24 | 453.0 | 227.0 | 16.4 | 0.67 |

[a] Aerosol optical depth ($\tau$), $\alpha$ and $\beta$ correspond to 18 December while the other properties are for 7 December. Aerosol optical depth measurements could not be conducted on 7 December. $\beta_{sca}$ and $\beta_{abs}$ are expressed in units of M $m^{-1}$ ($10^6$ $m^{-1}$), and BC mass is expressed in unit of $\mu g$ $m^{-3}$

in MODIS level-3 aerosol optical depth maps (Fig. 2f, g). Aerosol optical depth over most of western India is $\leq$0.2 on 7 December, a calm day (Fig. 2f), which increases by at least fourfold on 26 December, a hazy/smoky day (Fig. 2g).

Airmass back-trajectory analysis at different heights are performed to investigate the source regions and the transport pathways of pollutants before they reach the measurement location. A 7-day back-trajectory analysis is performed considering the average residence time of aerosols in the lower atmosphere, which is about a week. Air back-trajectory for Ahmedabad on 7 (clear) and 26 (haze/smoke) December at 10-, 100-, 500-, 1000-, 2500- and 5000-m heights are calculated (Fig. 3b, c) using the HYSPLIT model (Draxler and Hess 1998). Surface effects can influence the back-trajectory at 10-m, however surface effects on trajectories are minimal, given that back-trajectories for 10- and 100-m heights are identical (Fig. 3b, c). An analysis of aerosol extinction coefficient profiles and columnar aerosol optical depths measured over Ahmedabad revealed that aerosol extinction from the surface up to 5000-m altitude contributes >98% to the columnar aerosol optical depth during the year (Ramachandran and Kedia 2010). Further, aerosol extinction from the surface to 2 km contributes about 86% in winter. The airmasses that contribute most to aerosol concentration have spent all the time within the mixed layer on both days (Fig. 3b, c). Since, the airmasses have spent a significant portion of the last two to three days within the mixed layer they are likely to be representative of surface sources. On 7 December, the airmasses near the surface are more regional and are from north/north-west India, where aerosol optical depths are low (Fig. 2f); above 500 m the flow originates and travels above arid regions (regions of small aerosol optical depths, Fig. 2f), while on 26 December the airmasses originate over east India and traverse over urban and industrialized locations (regions of high aerosol optical depths, Fig. 2g) before reaching Ahmedabad. During other days in December the airmasses are found to originate and pass above north or west of Ahmedabad (not shown). Thus, strong descent, and variation in the origin of the airmass (regions of high aerosol optical depths) accompanied with haze and smoke, gave rise to higher aerosol optical depths during 24–26 December.

### 4.2 Surface Aerosol Features

The aerosol scattering coefficient ($\beta_{sca}$) on 7 December is less than 100 M $m^{-1}$ ($10^6$ $m^{-1}$) most of the day, and is marked with two peaks occurring around 0730 and 2100 local time respectively, when $\beta_{sca}$ values are higher than 150 M $m^{-1}$ (Fig. 4a). On 26 December $\beta_{sca}$ values are higher throughout the day (Fig. 4a); however, the magnitude of increase in $\beta_{sca}$

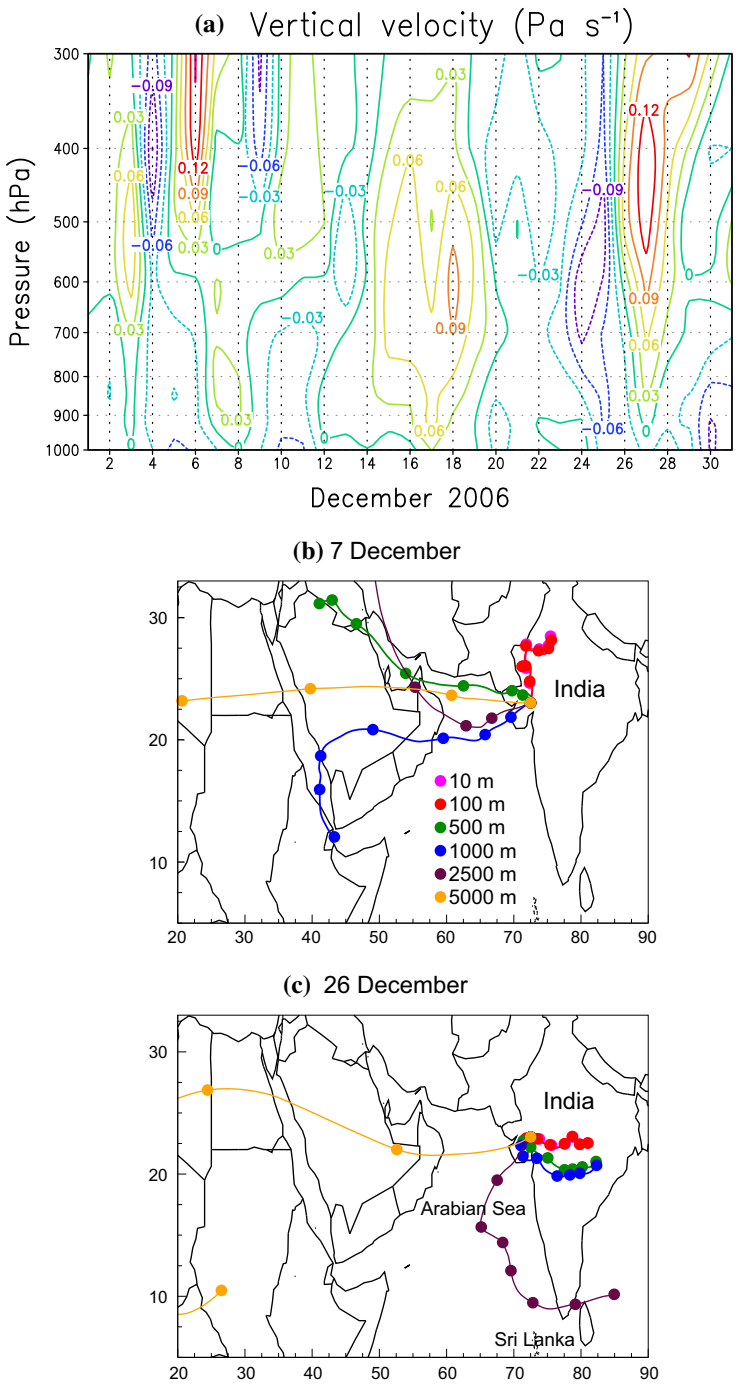


**Fig. 3** **a** Vertical velocity for the month of December 2006 over Ahmedabad from 1000 hPa (surface) to 300 hPa (≈9 km). **b** and **c** show the 7-day back-trajectory on 7 and 26 December, respectively, for Ahmedabad at 10-, 100-, 500-, 1000-, 2500- and 5000-m heights. The back-trajectory is plotted at 1-h interval. The symbols are shown at 24-h interval

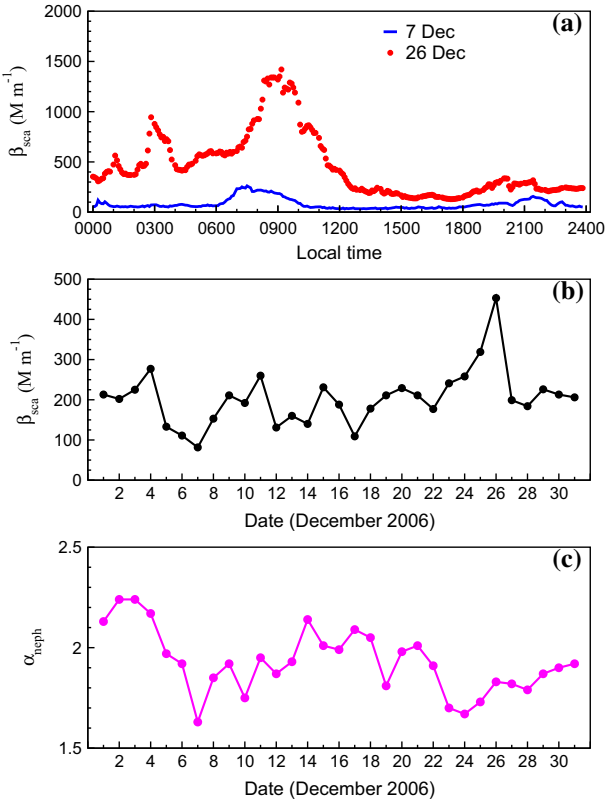


**Fig. 4** **a** Diurnal evolution of 550 nm $\beta_{sca}$ over Ahmedabad on 7 and 26 December 2006. **b** and **c** show the daily mean $\beta_{sca}$ and $\alpha_{neph}$ over the month of December 2006

on 26 December with respect to 7 December shows variation. The $\beta_{sca}$ value is more than an order of magnitude higher on 26 December at around 0900 local time. Values of $\beta_{sca}$ are about 2–4 times higher during 2000–2400 local time on 26 December compared to 7 December. On 26 December $\beta_{sca}$ values are not only higher but also the diurnal variation is different compared to 7 December, which gives rise to significant diurnal differences. The higher $\beta_{sca}$ values on 26 December occur despite the fact that the measured $\beta_{sca}$ are corrected for relative humidity effects, suggesting a substantial increase in the surface concentration of scattering aerosols on 26 December.

A significant increase in aerosol concentrations at the surface and in the column (Fig. 2a) are seen over Ahmedabad when the flow is easterly and when airmasses originate from central India (Fig. 3c). Monthly mean $\beta_{sca}$ over Ahmedabad is found to be significantly higher (Table 3) than the rural continental and remote coastal/marine locations in USA, confirming the presence of large amounts of scattering aerosols over Ahmedabad.

Daily mean $\alpha_{neph}$ values estimated from $\beta_{sca}$ (Fig. 4c) are in the range of 1.6–2.2 over Ahmedabad during December 2006; $\alpha$ is 1.63 (lowest, Fig. 4c) on 7 December, while it is higher on 26 December with a value of 1.83. Higher $\alpha$ values indicate the dominance of smaller size aerosols compared to larger aerosol particles, which is supported by a high $\beta_{sca}$ (Table 2). Values of $\alpha_{neph}$ and $\beta_{sca}$ are higher on 26 December suggesting a significant increase in the amount of sub-micron aerosols compared to 7 December.

**Table 3** Comparison of mean aerosol optical properties obtained during December 2006 over Ahmedabad with the 3-year (1997–1999) median values obtained over rural continental and remote coastal/marine surface stations in the USA

| Location | $\beta_{sca}$ ($Mm^{-1}$) | $\beta_{abs}$ ($Mm^{-1}$) | $\alpha_{neph}$ | *SSA* | *b* | *g* |
|---|---|---|---|---|---|---|
| Ahmedabad | 204 | 125.5 | 1.93 | 0.61 | 0.16 | 0.53 |
| Southern Great Plains, Oklahoma | 27 | 1.3 | 2.34 | 0.94 | 0.12 | 0.61 |
| Bondville, Illinois | 39 | 3.3 | 2.38 | 0.92 | 0.12 | 0.61 |
| Sable Island, Nova Scotia | 9.6 | 1.0 | 2.29 | 0.90 | 0.13 | 0.58 |
| Barrow, Alaska | 4.7 | 0.2 | 1.62 | 0.96 | 0.11 | 0.63 |

Black-carbon mass concentrations on 7 December are found to be $\leq 5$ $\mu g\ m^{-3}$ before 0600 local time and starts increasing thereafter (Fig. 5a). Black-carbon mass decreases after 0830 local time, remaining constant until 1800 local time, similar to the diurnal variation in $\beta_{sca}$ (Fig. 4a). Black-carbon mass concentrations increase after 1800 and are in the 5–7 $\mu g\ m^{-3}$ range during 1900–2100 local time. Black-carbon mass concentrations are higher on 26 December. It should be noted that both 7 (Thursday) and 26 December were weekdays. In Ahmedabad the black-carbon diurnal variations were similar on weekdays and weekends (Bapna et al. 2013). Black-carbon mass concentrations on 26 December are found to rise about an hour later (after 0700 local time), than 7 December. Black-carbon mass concentrations and $\beta_{abs}$ on 26 December are about four times higher than those measured on 7 December (Table 2). Similar variations in $\beta_{sca}$ values are seen on 7 and 26 December including the occurrence of delayed peak in $\beta_{sca}$ on 26 December, however, the $\beta_{sca}$ on 26 December is about six times higher than 7 December (Table 2).

On a typical (normal) day in an urban location the surface aerosol characteristics are found to exhibit a diurnal variation marked with two peaks: one in the morning hours just after the sunrise and the other in the evening hours. Over Ahmedabad the peaks in aerosol concentrations were found to occur between 0700–0900 and 1900–2100 local time (Ramachandran and Rajesh 2007). The peak in the morning arises due to an accumulation of local morning domestic and traffic emissions in the shallow stable mixed layer that then becomes diluted as convective mixing develops. Then, the aerosol concentration decreases due to an increase in the mixed-layer height (Figs. 1d, 4a). An increase in emissions from road traffic accompanied with a decreasing mixed-layer height result in a second maxima in aerosol properties in the late evening hours (Fig. 5a). Diurnal variations in surface aerosols over Ahmedabad exhibit a good correspondence with the mixed-layer height and anthropogenic activities.

Both $\beta_{sca}$ and black-carbon mass concentrations are higher on 26 December to start with due to the shallow mixed layer in midnight hours, and conditions of haze and smoke the previous evening. With daybreak the local aerosol emissions from anthropogenic activities over Ahmedabad increase, which results in higher aerosol loading in the 0700–1100 period. The hazy conditions accompanied with airmass descent (Fig. 3a) and transport (Fig. 3c) resulted in higher levels of aerosol loading near surface as well as in the column on 26 December. Hourly mean relative humidity values were high ($> 60\%$ going up to 80%) in the morning hours on 26 December. As the day progressed the atmospheric conditions become clearer, relative humidity decreased (30–40%) and the aerosols get ventilated, thus, resulting in lower $\beta_{sca}$ and black-carbon mass concentrations during 1300–1500 local time. Daily mean black-carbon mass concentration is found to be the lowest on 7 December at 4.3 $\mu g\ m^{-3}$ and the highest black-carbon mass is found on 26 December with a value of 16.4 $\mu g\ m^{-3}$ (Fig. 5b, Table 2). The daily mean black-carbon mass variation (Fig. 5b) is similar to the variation

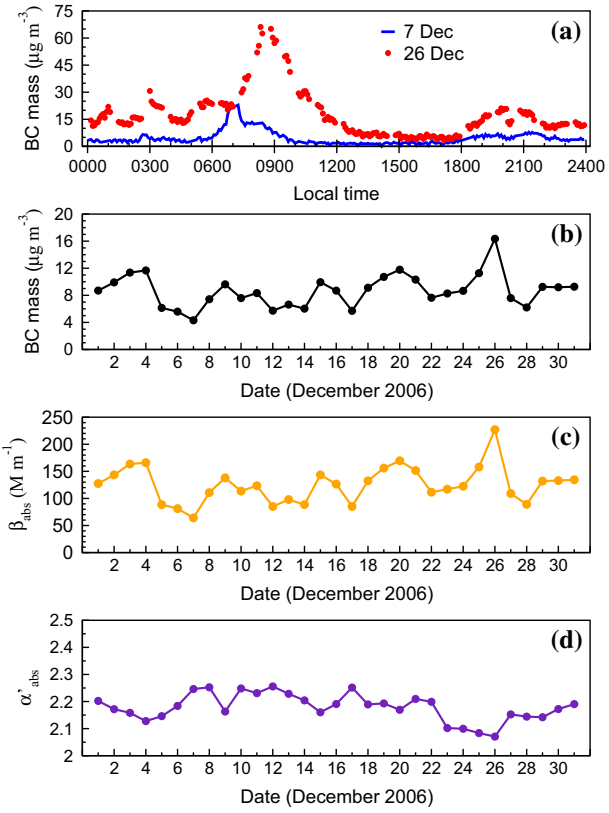


**Fig. 5** **a** Diurnal variation in black-carbon (BC) mass concentrations measured over Ahmedabad on 7 and 26 December 2006. The remaining panels show the daily mean values of black-carbon mass concentration (**b**), $\beta_{abs}$ at 555 nm (**c**), and $\alpha'_{abs}$, a measure of spectral aerosol absorption (**d**)

in $\beta_{sca}$ (Fig. 4b). $\alpha'_{abs}$ is found to be in the range of 2.07 and 2.25 over Ahmedabad during December 2006 (Fig. 5d). The low (2.07 on 26 December) and high (2.25 on 7 December) $\alpha'_{abs}$ values are above the $\pm 1\sigma$ from the monthly mean value of 2.18. $\alpha'_{abs}$ tending closer to 2 on 26 December suggests a relative increase in the amount of black-carbon aerosols emitted from fossil-fuel burning compared to 7 December.

The single-scattering albedo on 7 December is lower than 26 December from 0100 to 0900 local time (Fig. 6a). During the rest of the day *SSA* on 26 December is either comparable to 7 December values or is higher. The diurnal mean single-scattering albedo on 7 and 26 December is 0.56 and 0.67 respectively (Table 2). The single-scattering albedo depends on the chemical composition of aerosols present in the aerosol distribution, and consequently on the relative contributions of scattering and absorption due to aerosols (Table 1). A higher single-scattering albedo indicates the dominance of scattering aerosols than absorbing aerosols. The single-scattering albedo is in the 0.56–0.67 range over Ahmedabad during December 2006 (Fig. 6b). Higher $\beta_{abs}$ (Fig. 5c), and lower single-scattering albedo (Fig. 6b) obtained over Ahmedabad compared to rural continental and remote coastal/marine locations in USA (Table 3) suggests the dominance of absorbing aerosols in Ahmedabad.

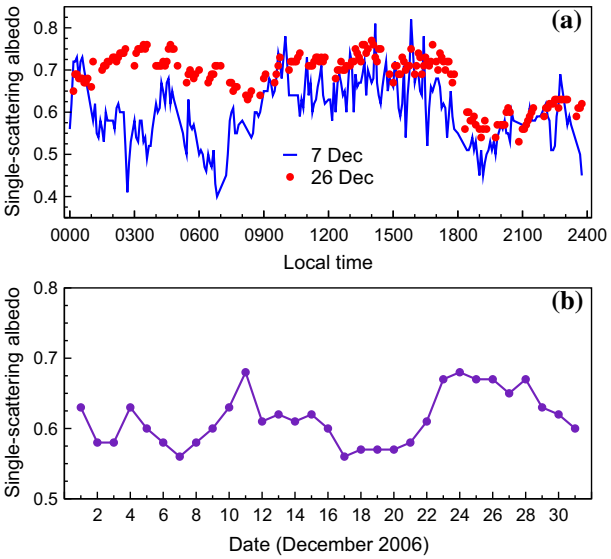


**Fig. 6** **a** Diurnal variation of single-scattering albedo at 550 nm on 7 and 26 December 2006. **b** Daily mean single-scattering albedo during the month of December 2006

The hemispheric backscatter fraction $b$ is higher on 7 December compared to 26 December (Fig. 7a, b). The daily mean backscatter fraction is in the 0.13–0.18 range over Ahmedabad during December 2006. The monthly mean $b$ is higher than the median $b$ values obtained over rural continental and remote coastal/marine locations in the USA (Table 3). The monthly mean $b$ value during 1996–2000 over the Southern Great Plains, Oklahoma was found to be in the 0.10–0.15 range; the annual mean $b \approx 0.13$. The value of $b$ was found to decrease in midsummer which was attributed to the increase in the fraction of larger particles (Sheridan et al. 2001) over the Southern Great Plains. Mean $b$ values were estimated to be 0.131, 0.115, and 0.137 for the biomass burning aerosols at Cuiabá, Porto Velho, and Marabá in the Amazon basin (Kotchenruther and Hobbs 1998). The higher $b$ values in Ahmedabad indicate the dominance of fine-size aerosols in this region. The values of the asymmetry parameter $g$ over Ahmedabad are higher on 26 December than on 7 December (Fig. 7c, d). Daily mean $g$ values are in the 0.45–0.6 range and the monthly mean $g$ is 0.53 (Table 3). The parameter $g > 0.6$ over rural continental and remote coastal/marine surface stations in the USA (Table 3). The lower $g$ and higher $b$ and $\alpha_{\text{neph}}$ values over Ahmedabad confirm that smaller aerosol particles dominate the size distribution in this region.

### 4.3 Surface Versus Column Aerosols: Variation and Contribution

The variations in surface aerosols are consistent with column variations (Figs. 2, 4, 5). The contribution of surface aerosol characteristics to column aerosol properties can be estimated using aerosol extinction and optical depth, and by deriving aerosol scale height. The columnar aerosol optical depth ($\tau$) can be derived by integrating the aerosol extinction coefficient ($\beta_{\text{ext}}$) obtained as a function of altitude $z$, as

$$\tau = \int_{z_0}^{z_{\max}} \beta_{\text{ext}}\, \mathrm{d}z, \tag{2}$$

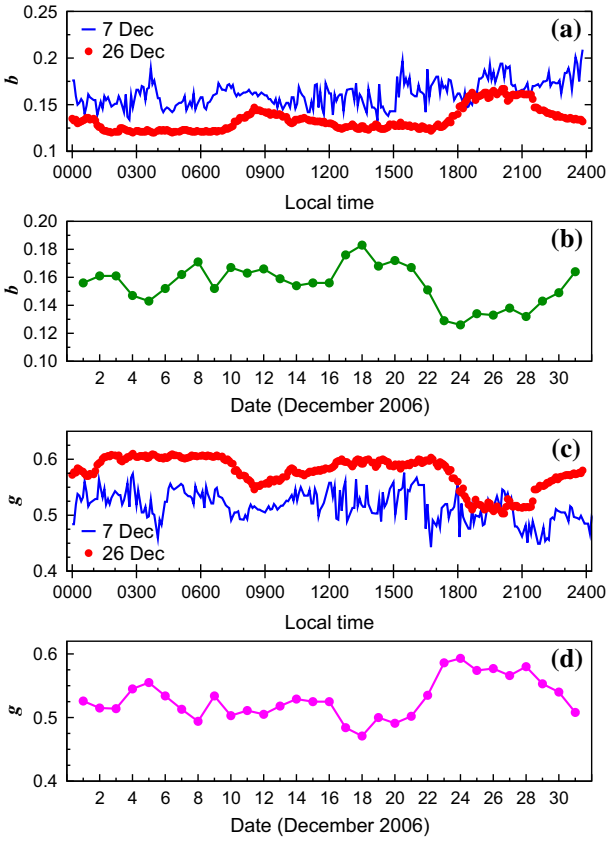


**Fig. 7** Diurnal variation of the hemispheric backscatter fraction, $b$ (**a**) and asymmetry parameter, $g$ (**c**) over Ahmedabad on 7 and 26 December 2006. **b** and **d** show the corresponding daily mean values over the month of December

where $z_0$ and $z_{max}$ correspond to surface and the maximum altitude up to which the aerosols exist. Based on the above equation which connects surface and columnar aerosol properties, the aerosol scale height can be estimated. The aerosol scale height ($H$), which represents the characteristic vertical distribution of aerosols, can be written as

$$H = \frac{\tau}{\beta_{ext}(z = 0)}. \tag{3}$$

The scale height is obtained using the daily mean MODIS level-2 and level-3 550-nm aerosol optical depths (Fig. 8a), and $\beta_{ext}(= \beta_{sca} + \beta_{abs})$ measured over Ahmedabad (Figs. 4b, 5c). This was done as MODIS aerosol optical depths (level-2 and level-3) (Fig. 2) and $\beta_{ext}$ correspond to the same wavelength, and were available for all the 31 days in December 2006. The magnitude of the scale height estimated in this manner provides information on the contribution of near surface aerosols to the columnar characteristics. A higher value of scale height suggests a lesser contribution from the surface, while a lower value indicates the dominance of contribution from the surface.

The aerosol scale height values (Fig. 8a) exhibit similar variations to that of the MODIS level-2 and level-3 aerosol optical depths (Fig. 2a). Aerosol scale heights determined using

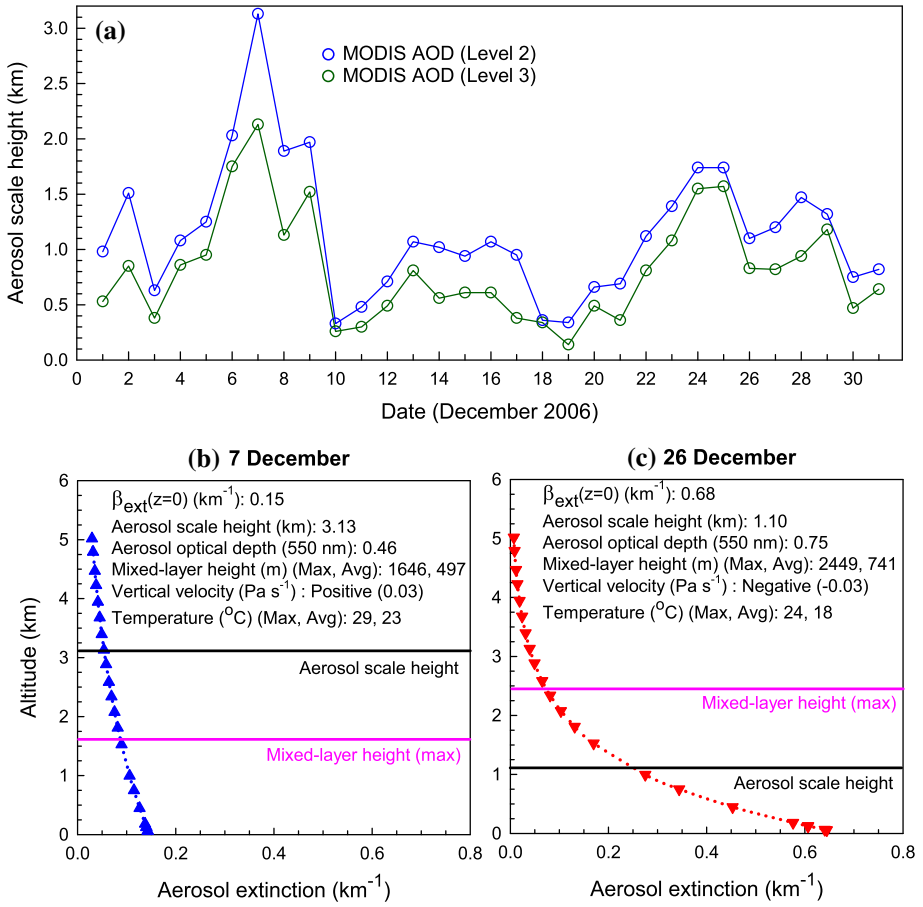


**Fig. 8** **a** Aerosol scale height ($H$) (Eq. 3) derived using $\beta_{sca}$, $\beta_{abs}$ and MODIS level-2 and level-3 aerosol optical depths. **b** and **c** show aerosol characteristics and atmospheric parameters for 7 and 26 December 2006, respectively. Parameters shown include the aerosol extinction at the surface ($\beta_{ext}$ at $z = 0$), aerosol scale height (km), aerosol optical depth, maximum and average values of the mixed-layer height (m) and temperature (°C), and vertical velocity (Pa $s^{-1}$). These days were selected because they represent the lowest (7 December) and highest (26 December) surface aerosol amounts

MODIS level-2 aerosol optical depths are larger than those derived using MODIS level-3 aerosol optical depths (Fig. 8a), because level-2 aerosol optical depths are comparatively larger than level-3 aerosol optical depths (Fig. 2a). The scale height on 7 December is 3.13 km (level-2 aerosol optical depth) and 2.13 km (level-3 aerosol optical depth), while on 26 December the scale heights are 1.10 and 0.83 km for level-2 and level-3 aerosol optical depths respectively. The monthly mean ($\pm 1\sigma$) aerosol scale height for December 2006 is 1.15 ($\pm$0.60) km (level-2 aerosol optical depths), and 0.82 ($\pm$0.48) km (level-3 aerosol optical depths) indicating a dominant contribution of near surface aerosols to the column. The aerosol scale height on 26 December is smaller than the December mean confirming that the higher near surface aerosol concentration (Table 2) obtained on that day indeed dominates the columnar aerosol content. A regression between the surface extinction and columnar aerosol optical depths yielded a higher correlation coefficient of 0.6.

Using the scale height the altitude profiles of aerosol extinction are derived following

$$\beta_{\text{ext}}(z) = \beta_{\text{ext}}(z = 0)\ \exp(-z/H), \tag{4}$$

where $\beta_{\text{ext}}$ $(z)$ is the aerosol extinction ($\text{km}^{-1}$) at altitude $(z)$, $\beta_{\text{ext}}$ $(z= 0)$ is the aerosol extinction ($\text{km}^{-1}$) at the surface ($\beta_{\text{sca}} + \beta_{\text{abs}}$), and $H$ is the aerosol scale height. Since the surface aerosol characteristics were the lowest and highest on 7 and 26 December respectively, aerosol characteristics and atmospheric parameters pertaining to these two days are shown (Fig. 8). The influence of variations in meteorological parameters on aerosol characteristics can be distinctly seen on 7 and 26 December (Fig. 8b, c). The average surface temperature is higher on 7 December which results in a mixed-layer height that is lower by 800 m (Fig. 8) compared to 26 December; the difference in mixed-layer height on these days is much higher than the errors in deriving the mixed-layer height. The vertical velocity is positive indicating rising motion and faster dispersal of aerosols on 7 and 18 December giving rise to lower surface and columnar values (Figs. 2a, 3a), while on 26 December the vertical velocity is negative leading to sinking motion of air parcels which results in higher values of surface and columnar aerosol concentrations.

## 5 Summary and Conclusions

Aerosols exhibit a unique character over urban regions where the type and amount of aerosol emissions vary significantly compared to remote continental, rural, and oceanic regions. Urban aerosols can also be modulated by the variations in relative humidity, mixed-layer height, and mesoscale vertical velocity. However, it is a formidable task to delineate the contribution of local and remote sources of aerosols and their types depending on the regions from where the aerosols are transported, wind speeds, mixing-layer height, and vertical velocity variations to the aerosol characteristics measured over urban region. Studies connecting the above features and aerosol characteristics are quite rare. For the first time, the influence of variations in relative humidity, mixed-layer height, and mesoscale vertical velocity on aerosol characteristics over an urban region are investigated.

The major conclusions are:

(1) Aerosol optical depths are found to be in the 0.2–0.6 range during 1–20 December over Ahmedabad (clear conditions), and >0.75 on 26 December (haze/smoke). MODIS level-2 (10-km × 10-km resolution) and level-3 (1° × 1° resolution) aerosol optical depths agree well with the in situ ground-based aerosol optical depths measured by the Sun photometer; MODIS level-3 aerosol optical depths are consistently lower than level-2 aerosol optical depths. The Ångström wavelength exponent $\alpha$ varies from 1.5 to 2 during 1–17, and 19–31 December; it was lowest on 18 December with a value of 1.1. The aerosol columnar loading $\beta$ tracks the aerosol optical depth variation quite well. Aerosol optical depth, $\alpha$ and $\beta$ are higher on 26 December than 18 December indicating a significant increase in the amount of sub- and super-micron aerosols on 26 December.

(2) Aerosol scattering coefficient ($\beta_{\text{sca}}$), black-carbon mass concentrations and aerosol absorption coefficient ($\beta_{\text{abs}}$) are low on 7 December (clear-sky conditions) and high on 26 December (haze/smoke conditions). $\beta_{\text{sca}}$ and black-carbon mass concentrations are higher on 26 December from midnight onwards, affecting the consequent diurnal evolution of these parameters. The rates of increase of $\beta_{\text{sca}}$, black-carbon mass, and $\beta_{\text{abs}}$ on 26 December compared to 7 December varied throughout the day; $\beta_{\text{sca}}$ is higher

by a factor of 6 on 26 December compared to 7 December, while black-carbon mass concentration and $\beta_{abs}$ are about four times higher on 26 December than on 7 December.

(3) Daily mean $\alpha_{neph}$ values estimated from $\beta_{sca}$ at 450, 550 and 700 nm are found to be in the 1.6–2.2 range in December 2006. Values of $\alpha_{neph}$ on 26 December are higher than 7 December suggesting the presence of more number of fine-mode aerosols on 26 December. The mean spectral dependence of aerosol absorption indicated by $\alpha'_{abs}$ is found to be $2.18 \pm 0.05$ for December 2006. The value of $\alpha'_{abs}$ is found to be the lowest on 26 December (2.07) and the highest on 7 December (2.25); the spectral absorption exponent $\alpha'_{abs} > 2$ suggests the dominance of black-carbon aerosol emissions, from biomass burning. The dominant contribution from biomass/biofuel emissions to carbonaceous aerosols over an urban location, as seen in Ahmedabad, can occur as people burn dry leaves, shrubs, paper and waste materials during cold winter. This result over an urban location is rather unexpected as conventionally fossil fuel emissions, which produce strongly light absorbing carbonaceous particles, dominate the urban regions.

(4) The single-scattering albedo is 0.56 on 7 December and 0.67 on 26 December. A higher single-scattering albedo on 26 December occurs due to the dominance of scattering aerosols in the aerosol size distribution as single-scattering albedo depends crucially on the ratio of scattering and absorbing aerosols. Single-scattering albedo is in the 0.56–0.67 range over Ahmedabad. Aerosol absorption coefficient is higher, and single-scattering albedo is lower in Ahmedabad compared to the rural continental and remote marine/coastal stations in the USA. This comparison reveals on a day-to-day basis depending on the variation in the amount of scattering and absorbing aerosols single-scattering albedo can be high or low, and that absorbing aerosols dominate the aerosol size distribution above Ahmedabad as compared to other locations.

(5) The hemispheric backscatter fraction ($b$) is found to lie in the 0.13–0.18 range over Ahmedabad during December 2006. The monthly mean $b$ over Ahmedabad is higher than those obtained over rural continental and remote marine/coastal surface stations in USA. Asymmetry parameter ($g$) is found to be low and is in the 0.45–0.6 range; the monthly mean $g$ is 0.53. Higher $b$ and $\alpha_{neph}$, and lower $g$ values indicate the dominance of smaller particles in the aerosol size distribution.

(6) Atmospheric conditions on 7 and 26 December were distinctly different; 7 December was characterized by a clear atmosphere, a smaller mixed-layer height, positive vertical velocity and higher aerosol scale height (>3 km), while 26 December was marked with hazy and smoky conditions, a greater mixed-layer height, negative vertical velocity and lower aerosol scale height ($\approx$1 km). These atmospheric conditions lead to lower, and higher values of surface and columnar aerosol concentrations on 7 and 26 December respectively.

Our study quantitatively documents the influence of relative humidity, mixed-layer height, and mesoscale vertical velocity variations on aerosol characteristics over an urban region, the results of which can serve as inputs in modeling the radiative and climate impact of aerosols. The findings over an urban region on the relative increase in scattering and absorbing aerosols due to variations in relative humidity, mixed-layer height, and mesoscale vertical velocity between clear and hazy days, the dominance of fine-mode particles, and contribution of biomass-burning emissions vis-à-vis fossil-fuel emissions to aerosols are unique, and can be utilized to compare/contrast and understand better the different processes that influence aerosol characteristics. The significant variations in aerosol characteristics as functions of time (day-to-day, clear to hazy) and altitude (surface vs. column) have crucial consequences on the Earth-atmosphere radiation budget and hydrological cycle on regional scales.

**Acknowledgements** We thank ISRO-GBP, ISRO Headquarters, Bengaluru for partial funding support. Daily mean temperature and wind speed data are obtained from NOAA, NESDIS National Climatic Data Center, USA. Diurnal relative humidity data over Ahmedabad are downloaded from http://www.wunderground.com. MODIS level-3 aerosol optical depths are downloaded using NASA Goddard Earth Sciences Data and Information Services Center's Interactive Online Visualization and Analysis Infrastructure. MODIS level-2 aerosol optical depth data are acquired from LAADS-DAAC located in the GSFC (https://ladsweb.nascom.nasa.gov). Vertical velocity for December 2006 was obtained from the NOAA-ESRL Physical Sciences Division, Boulder, Colorado from their web site at http://www.cdc.noaa.gov/. The authors gratefully acknowledge the NOAA Air Resources Laboratory (ARL) for the provision of the HYSPLIT transport and dispersion model and READY website (http://www.ready.noaa.gov) used in this publication.

## References

Anderson TL, Ogren JA (1998) Determining aerosol radiative properties using the TSI 3563 integrating nephelometer. Aerosol Sci Technol 29:57–69

Anderson TL, Covert DS, Marshall SF, Laucks ML, Charlson RJ, Waggoner AP, Ogren JA, Caldow R, Holm RJ, Quant FR, Sem GJ, Wiedensohler A, Ahlquist NA, Bates TS (1996) Performance characteristics of a high-sensitivity, three-wavelength total scatter/backscatter nephelometer. J Atmos Ocean Technol 13:967–986

Andrews E, Sheridan PJ, Fiebig M, McComiskey A, Ogren JA, Arnott P, Covert D, Elleman R, Gaspirini R, Collins D, Jonsson H, Schmid B, Wang J (2006) Comparison of methods for deriving aerosol asymmetry parameter. J Geophys Res 111:D5

Bapna M, Sunder Raman R, Ramachandran S, Rajesh TA (2013) Airborne black carbon concentrations over an urban region in western India—temporal variability, effects of meteorology, and source regions. Environ Sci Pollut Res 20:1617–1631

Bodhaine BA (1995) Aerosol absorption measurements at Barrow, Mauna Loa and the south pole. J Geophys Res 100:8967–8975

Charlson RJ, Covert DS, Larson TV (1984) Observation of the effect of relative humidity on light scattering by aerosols. In: Ruhnke LH, Deepak A (eds) Hygroscopic aerosols. Deepak Publishing, Hampton, pp 35–44

Clarke AD, Howell S, Quinn PK, Bates TS, Ogren JA, Andrews E, Jefferson A, Massling A, Mayol-Bracero O, Maring H, Savoie D, Cass G (2002) INDOEX aerosol: a comparison and summary of chemical, microphysical, and optical properties observed from land, ship, and aircraft. J Geophys Res 107:8033

Draxler R, Hess GD (1998) An overview of the HYSPLIT-4 modeling system for trajectories, dispersion and deposition. Aust Meteorol Mag 47:295–308

Hegg DA, Covert DS, Rood MJ, Hobbs PV (1996) Measurements of aerosol optical properties in marine air. J Geophys Res 101:12893–12903

Hess M, Koepke P, Schult I (1998) Optical properties of aerosols and clouds: the software package OPAC. Bull Am Meteorol Soc 79:831–844

Kalnay E, Kanamitsu M, Kistler R, Collins W, Deaven D, Gandin L, Iredell M, Saha S, White G, Woollen J, Zhu Y, Chelliah M, Ebisuzaki W, Higgins W, Janowiak J, Mo KC, Ropelewski C, Wang J, Leetmaa A, Reynolds R, Jenne R, Joseph D (1996) The NCEP/NCAR 40-year reanalysis project. Bull Amer Meteorol Soc 77:437–471

Kedia S, Ramachandran S (2011) Seasonal variations in aerosol characteristics over an urban location and a remote site in western India. Atmos Environ 45:2120–2128

Kirchstetter TW, Novakov T, Hobbs PV (2004) Evidence that the spectral dependence of light absorption by aerosols is affected by organic carbon. J Geophys Res 109:D21208

Kotchenruther RA, Hobbs PV (1998) Humidification factors of aerosols from biomass burning in Brazil. J Geophys Res 103:32081–32089

Pasricha PK, Gera BS, Shastri S, Maini HK, Ghosh AB, Tiwari MK, Garg SC (2003) Role of the water vapor greenhouse effect in the forecasting of fog occurrence. Boundary Layer Meteorol 107:469–482

Ramachandran S, Kedia S (2010) Black carbon aerosols over an urban region: radiative forcing and climate impact. J Geophys Res Atmos 115:D10

Ramachandran S, Kedia S (2011) Aerosol radiative effects over an urban location and a remote site in western India: seasonal variability. Atmos Environ 45:7415–7422

Ramachandran S, Rajesh TA (2007) Black carbon aerosol mass concentrations over Ahmedabad, an urban location in western India: comparison with urban sites in Asia, Europe, Canada and USA. J Geophys Res 112:D06211

Ramachandran S, Rengarajan R, Jayaraman A, Sarin MM, Das SK (2006) Aerosol radiative forcing during clear, hazy and foggy conditions over a continental polluted location in north India. J Geophys Res 111:D20214

Remer LA, Kleidman RG, Levy RC, Kaufman YJ, Tanré D, Mattoo S, Martins V, Ichoku C, Koren I, Yu H, Holben BN (2008) Global aerosol climatology from the MODIS satellite sensors. J Geophys Res 113:D14S07

Sheridan PJ, Delene DJ, Ogren JA (2001) Four years of continuous surface aerosol measurements from the Department of Energy's Atmospheric Radiation Measurement Program Southern Great Plains Cloud and Radiation Testbed site. J Geophys Res 106:20735–20747

Stull RB (1988) An introduction to boundary layer meteorology. Kluwer, Dordrecht

Wiscombe WJ, Grams G (1976) The backscattered fraction in two-stream approximations. J Atmos Sci 33:2440–2451

## Affiliations

**S. Ramachandran[1] · T. A. Rajesh[1] · Sumita Kedia[2]**

T. A. Rajesh
rajeshta@prl.res.in

Sumita Kedia
sumitag@cdac.in

1 Space and Atmospheric Sciences Division, Physical Research Laboratory, Ahmedabad 380009, India

2 Centre for Development of Advanced Computing, Pune 411008, India